Experimental and Theoretical Study of the Acidic Degradation of Poly(2,2′-dioxy-1,1′-biphenyl)phosphazene

Gabino A. Carriedo,* Francisco J. García Alonso, Jose L. García Álvarez, and Alejandro Presa Soto

Departamento de Química Orgánica e Inorgánica, Facultad de Química, Universidad de Oviedo, Oviedo 33071, Spain

M. Pilar Tarazona, M. Teresa R. Laguna, Gema Marcelo, Francisco Mendicuti, and Enrique Saiz*

Departamento de Química Física, Universidad de Alcalá. 28871, Alcalá de Henares, Spain

Received July 10, 2008; Revised Manuscript Received September 9, 2008

ABSTRACT: Poly(2,2′-dioxy-1,1′-biphenyl)phosphazene (**I**) is a weak base that can be reversibly protonated with HBF_4 in acetone. Acidic degradation of poly(2,2′-dioxy-1,1′-biphenyl)phosphazene was experimentally performed using HBF_4, HCl, and H_2SO_4 yielding the same polymer I with lower molecular weights. The reaction takes place through protonation of some of the skeletal bonds thus producing a protonated P^+-NH bond, and posterior rupture of those bonds by reaction with water. The hydrolysis breaks only these protonated skeletal bonds, leaving unaffected the regular P−N bonds. The degree of hydrolysis is controlled by the amount of time during which the system was treated with the acid. Molecular dynamics simulations performed on systems containing protonated and unprotonated oligomers together with water and HCl molecules proved that Cl^- ions and water molecules get close enough to protonated P^+−NH bonds as to produce a hydrolytical rupture, however, they do not get into such a proximity to the regular P−N bonds. The products of hydrolysis were characterized by (SEC−MALS) (i.e., size exclusion chromatography coupled with multiangle light scattering) and fluorescence. The results indicated that the parental polymer and all the degraded samples have the same chemical microstructure despite their very different molecular weight, i.e., they exhibit the same molecular calibration curve, unperturbed dimension, scaling law parameters, fluorescence emission, lack of cross-linking etc. It seems that the acidic degradation can be controlled to produce homogeneous samples in a much easier way than the thermal degradation used before.

Introduction

Polyphosphazenes are very interesting compounds in basic and applied material science.[1] In earlier works[2,3] we discovered that the reaction of $[NPCl_2]_n$ in THF with 2,2′-dihydroxy-1,1′-biphenyl ($HO-C_6H_4-C_6H_4-OH$) in the presence of K_2CO_3 occurred without cross-linking to give the linear and very soluble polyphosphazene having cyclic repeating units $[NP(O_2C_{12}H_8)]_n$ (**I**), with a M_w on the order of 10^6 (chart *1*), that had a very unusually high T_g (160 °C) for a phosphazene. Several studies showed that this polymer behaved as a random coil in solution[4] and that could be thermally degraded to lower M_w distributions.[4] The vibrational spectroscopy[5] and the rheological features of **I** have also been reported.[6]

A large variety of random copolymers combining biphenoxyphosphazene with other functionalized aryloxyphosphazene units (**II** in chart *1*) were prepared.[3] Those polymers also behave as random coils in solution,[7] and the functions R that were incorporated included amines,[8] esters,[9] carboxylic acids and polyamide chains,[10] and also ligands and their transition metal complexes.[11] Analogous thioaryloxy derivatives have also been prepared.[12] Some of the aryloxy-phosphazenes **II** were studied as nonlinear optical materials[13] and as imprinted polymers for recognitions of antibiotics.[14]

However, so far the chemical properties of the $[NP(O_2C_{12}H_8)]_n$ polymer have been little explored. Therefore, considering that the chemical functionalization of linear polyphosphazenes or their surfaces[15−17] is a very important subject and relevant to the design of materials with predetermined properties, we have initiated the study of the chemical reactivity of the $[NP(O_2C_{12}H_8)]_n$, starting by its basicity and reactions with protonic acids.

Chart 1

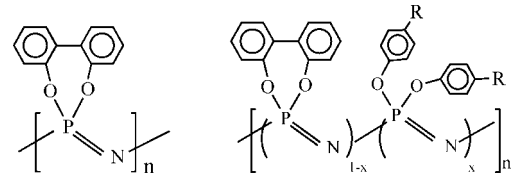

I **II**

Herein, we describe the acid base behavior of polyphosphazene **I**, the acid degradation to narrower distributions of controlled average M_w, and the solution properties of the new materials studied by size exclusion chromatography combined with multiangle light scattering, SEC−MALS[18] and fluorescence.[19] Molecular dynamics simulations of the system polymer−water−HCl, which were carried out trying to explain the hydrolytical process, are also depicted.

Experimental Section

All reactions were carried out under a dry N_2 atmosphere. The solvents were deoxygenated and dried following the standard methods. The HBF_4 (54% in diethyl ether), H_2SO_4 (98%) and HCl (37%) (Aldrich) were used as received.

Different samples of the polymer $[NP(O_2C_{12}H_8)]_n$ (**I**) were used in this study. All of them were prepared from $[NPCl_2]_n$ following the method described in reference,[20] and had very similar molecular

* Corresponding authors. (G.A.C.) Fax: + 34 985 103446. E-mail: gac@fq.uniovi.es. (M.P.T.) Fax: + 34918854763. E-mail: mpilar.tarazona@uah.es. (E.S.) E-mail: enrique.saiz@uah.es.

10.1021/ma8015568 CCC: $40.75
Published on Web 10/22/2008

weight distributions (GPC) with weight average molecular weights, M_w, in the range 0.5−0.8 10^6 and polydispersities indexes ($r = M_w/M_n$) around 3. The purity was always checked by C, H, N analysis, ^{31}P and ^1H NMR and IR spectroscopies. The T_g values were very near 160 °C for all samples.

The IR spectra were recorded with a Perkin-Elmer FT Paragon 1000 spectrometer. NMR spectra were recorded on Bruker AC-200, DPX-300 and Avance 300 instruments, using $CDCl_3$ as solvent unless otherwise stated. ^1H and $^{13}C\{^1H\}$ NMR are given in δ relative to TMS. $^{31}P\{^1H\}$ NMR are given in δ relative to external 85% aqueous H_3PO_4. Coupling constants are in Hz. C, H, N, analyses were performed with a Perkin-Elmer 240 microanalyzer. Chlorine analyses were performed by Galbraith Laboratories. GPC were measured with a Perkin-Elmer equipment with a Model LC 250 pump, a Model LC 290 UV, and a Model LC 30 refractive index detector. The samples were eluted with a 0.1% by weight solution of tetra-n-butylammonium bromide in THF through Perkin-Elmer PLGel (Guard, 10^5, 10^4 and 10^3 Å) at 30 °C. Approximate molecular weights were obtained by calibration using narrow molecular weight distribution polystyrene standards. Tg values were measured with a Mettler DSC 300 differential scanning calorimeter equipped with a TA 1100 computer.

The absolute molecular weight distributions and radii of gyration were determined by size exclusion chromatography, SEC, combined with multiangle laser light scattering, MALS. An OptiRex, interferometric refractometer from Wyatt Technology Corp was used as a concentration detector, RI, and a Dawn-DSP-F laser photometer also from Wyatt Technology Corp. was the mass and size detector used. A Model 510 pump (Waters), and a Rheodyne injector with a loop or 50 μL completed the equipment. Different sets of columns were tried and the best separation was obtained using two columns styragel HR5E and one column styragel HR6 (Waters). The eluent was the same as above. The Dawn photometer was calibrated with spectrometric grade toluene freshly distilled from sodium and benzophenone, and the normalization of the detectors was performed with standard monodisperse polystyrene of low molecular weight that did not show angular dependence on the light scattering signal. Standard monodisperse polystyrene was also used to determine the interdetector volume. The refractive index increments for the polymers were measured with a Brice-Phoenix differential refractometer at 436 and 546 nm and extrapolated to 632 nm using the Cauchy relationship. Tetrahydrofuran (THF) with a 0.1% tetra-*n*-butyl ammonium bromide was used as eluent. The solvents were filtered through a 0.2 μm Fluoropore membrane and degassed. The flow rate used was 1.0 mL/min and the temperature 25 °C.

Steady-state fluorescence measurements were performed on an SLM 8100 Aminco Spectrofluorimeter equipped with a Xe lamp, a double (single) concave grating monochromator at the excitation (emission) path and Glan-Thompson prism polarizers in both paths. The photomultiplier was cooled by a Peltier system. The excitation and emission slit widths were set to 16 nm. Right angle geometry, magic angle and rectangular 10 mm path cells were used for all fluorescence dilute solution measurements. The cell housing temperature (25 °C) was controlled by a thermostatic bath (Huber Ministat) and measured employing a Pt-100 probe with digital temperature processor (Nokeval model 2011). Solvent baselines were measured and subtracted from the spectra. The fluorescence decay measurements were achieved on a time-correlated single photon counting (TCSPC) FL900 Edinburgh Instruments spectrometer using as exciting power a nanoled (IBH) which emits at 280 nm. The system was equipped with two concave grating monochromators at both the excitation and emission paths and a red sensitive photomultiplier also immersed in a Peltier cooled housing. Slit bandwidths were 18 nm. So as not to attenuate the low fluorescence signal no polarizers were used in this case. Data acquisition was carried out by using a multichannel time detector and a time window width of 125 ns with a total of 10 000 counts at the intensity maximum. The instrumental response function was regularly obtained by measuring the scattering of a Ludox solution. Temperature was controlled by a bath (Techne TE-8A). Decay intensity profiles were fitted to a sum of exponential decay functions by the iterative reconvolution method.[21]

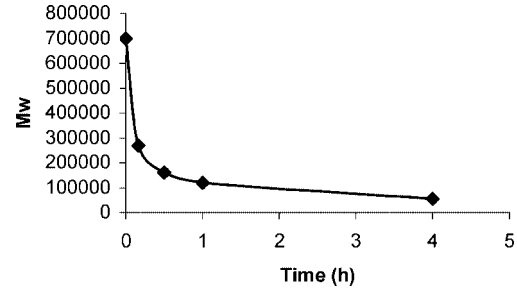

Figure 1. Average M_w (by GPC) of **I** as a function of the refluxing time in concentrated aqueous HCl.

Protonation of $[NP(O_2C_{12}H_8)]_n$ (I) with HBF_4. To a suspension of **I** (M_w = 700 000, r = 3.5) (2.0 g., 8.7 mmol) in acetone (50 mL), the acid HBF_4 (54% in diethyl ether) (1.5 mL, 10.93 mmol) was added in portions (0.25 mL, 1.82 mmol each time) at room temperature, and the mixture (that after the third addition was a clean solution, showing a signal in the ^{31}P NMR at −3.3 ppm) was stirred for 30 min. The final solution was poured dropwise into water (1 L) with stirring to give a precipitate that was washed with water (3 × 1 L), isopropyl alcohol and diethyl ether to give **I** as a white solid that was dried in vacuo at 70 °C for 3 days (yield 1.82 g, 91%). The spectroscopic data were identical to those of **I** and the analytical data found (62.2% C, 3.01% H, 6.01% N) showed a high purity (calculated 62.9% C, 3.52% H, 6.11% N). The new M_w was 400 000 with $r \approx 7.3$ (GPC). The T_g values (DSC) were in the range 159−162 °C.

Reaction of $[NP(O_2C_{12}H_8)]_n$ (I) with Aqueous HCl. A suspension of polymer **I** (M_w = 700 000, r = 3.5) (0.3 g., 1.30 mmol) in 40 mL of concentrated aqueous HCl acid (37%) was stirred at the refluxing temperature for a time t = 10 min., 30 min., 1 and 4 h. In each case the mixture was filtered and the solid was washed with water (until no acidic reaction), isopropyl alcohol and diethyl ether, and dried in vacuo at 70 °C for 2 days and over P_4O_{10} for 10 days to give the new distribution **Ia** to **Id** (yields 0.23−0.29 g, 77−97%). The spectroscopic data were identical to those of **I** and the analytical data found (**Ia**, t = 10 min, 60.3% C, 3.30% H, 5.72% N; **Ib**, t = 30 min, 61.5% C, 3.18% H, 5.70% N; **Ic**, t = 1 h, 60.8% C, 3.38% H, 5.83% N); and **Id**, t= 4 h, 61.4% C, 3.24% H, 5.76% N) showed a slight decrease in purity. The new M_w (GPC) values were as follows: **Ia**, 270 000 (r = 4.8); **Ib**, 160 000 (r = 3.5); **Ic**, 120 000 (r = 5.8); and **Id**, 55 000 (r = 31.4). The T_g values (DSC) were in the range 159−162 °C.

Prolonging the reflux for 17 h resulted in decomposition with the formation of biphenol, $NH_4(H_2PO_4)$ (identified by its IR and ^{31}P NMR spectra), and a white polymeric product containing **I** (yield 15%) as a broad distribution with M_w of 40 000 and a ^{31}P NMR spectrum showing the presence of cyclic and lineal small oligomers.

Reaction of $[NP(O_2C_{12}H_8)]_n$(I) with Aqueous H_2SO_4. The polymer **I** (M_w = 700 000, r = 3.5) (2.0 g., 8.7 mmol) was dissolved in 50 mL of concentrated (98%) sulfuric acid (^{31}P NMR sharp singlet at −0.2 ppm; ^1H NMR: broad multiplet with two maxima at −6.9 and −6.3 ppm) and the samples were stirred for a time t = 1 h, 24 h, 15 days, and 3 months. The mixture was poured slowly into water (1 L) and the precipitate was washed with water (3 × 1 L), isopropyl alcohol and diethyl ether and dried in vacuo at 70 °C for 3 days (yields 1.82−1.9 g, 91−95%). The spectroscopic data were identical to those of **I** and the analytical data found (t = 1 h: 62.2% C, 2.93% H, 5.98% N; t = 24 h: 61.7% C, 3.01% H, 5.83% N; t = 15 days: 61.7% C, 3.14% H, 6.00% N): t = 3 months, 60.0% C, 3.4% H, 5.68% N) showed a slight decrease in purity. The new M_w (GPC) values were as follows: t =1 h, 135 000 (r = 5.1); t = 24 h: 51 000 (r = 8.4); t = 15 days: 27 000 (r = 10.7); t = 3 months, 17 000 (r = 7.6). The T_g values (DSC) were in the range 159−162 °C.

Scheme 1

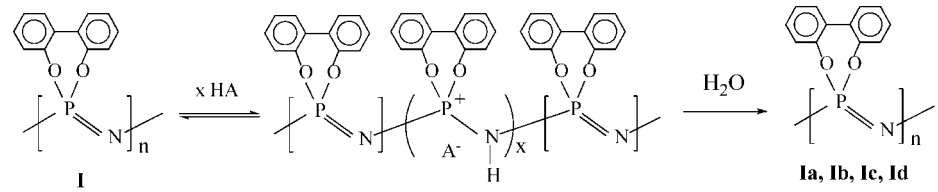

Results and Discussion

The addition of a small amount of HBF_4 (54% in diethyl ether) to a $CDCl_3$ solution of polymer **I** with a M_w of 720 000, caused turbidity and the ^{31}P NMR showed an increase of the chemical shift of the phosphazene phosphorus from −5.7 to −4.5 ppm. Further additions caused a white precipitate that was redissolved in the presence of NEt_3 to restore the initial chemical shift. Using acetone as solvent, however, where **I** is not soluble, the addition of different amounts of HBF_4 gave clear solutions. Their ^{31}P NMR spectra evidenced only a single signal for all the phosphorus with a chemical shift that increased with the amount of added acid reaching a maximum value of −3.3 ppm with exactly 1.0 equiv. Furthermore, the ^1H NMR spectra of the acetone solutions showed the well defined broad signal at 10.5 ppm, expected for the presence of PNHP protons.[22] These facts are consistent with the results of the protonation experiments observed with other basic polyphosphazenes.[22,23] Pouring the acidic acetone solutions into water gave a white precipitate of **I** that was recovered in more than 90% yield. The only noticeable change was the GPC chromatogram that was bimodal and showed a clear reduction of the average molecular weight to ca. 400 000 ($r = 7.3$).

A similar effect was observed by refluxing a suspension of **I** in concentrated aqueous hydrochloric acid (37% in weight), that led to a quantitative recovery of the polymer without any sign of chemical decomposition but having much lower average M_w. Various experiments showed that the M_w decreased with the refluxing time, very rapidly at the beginning but tending to a plateau (see Figure 1). Thus, the treatment of **I** with concentrated aqueous HCl for 10 min, 30 min, 1 h, or 4 h, allowed the quantitative preparation of polymers with different M_w distributions, **Ia** to **Id** respectively, and very high chemical purity (by ^{31}P and ^1H NMR and analysis) (Scheme 1 with HA = HCl and experimental part). The glass transition temperature of those lower M_w samples (160 °C) was practically that of the starting polymer **I**. A very similar reduction of M_w was observed during the thermal degradation of **I**, but the distributions obtained by heating were broader and with lower T_g values probably caused by the presence of decomposition products.[4]

We checked that the refluxing of **I** with pure water or with water in the presence of small amounts of HCl did not affect significantly the M_w, i.e., the HCl is not simply a catalyst for the chain degradation. Only after a prolonged reflux in aqueous HCl the chemical degradation of **I** took place. Thus, after 17 h, a small amount of **I** (M_w of ca. 40 000) mixed with lower linear and cyclic oligomers, including the triphosphazene $[N_3P_3(O_2C_{12}H_8)_3]$, some biphenol $HO-C_6H_4-C_6H_4-OH$, and the salt $(NH_4)H_2PO_4$ were recovered, showing the effects of extended hydrolysis. It is known that the related poly(diphenoxyphosphazene) does not undergo hydrolysis except at high temperatures unless the residual P−Cl bonds are abundant.[24] As the residual chlorine content in polymer **I** was extremely low (in the range of ppm), the slow hydrolysis might be helped by the effect of the HCl/water molecules over protonated skeletal bonds (see the next section for theoretical calculations trying to test this assumption).

As other polyphosphazenes,[16] **I** was soluble in sulfuric acid. Thus, the addition of **I** to concentrated sulfuric acid (98%) at room temperature gave viscous clear solutions, exhibiting an intense sharp peak at −0.2 ppm in the ^{31}P NMR spectrum and a broad multiplet with two maxima at −6.9 and −6.3 ppm in the ^1H NMR.

However, unlike the related poly(biphenoxyphosphazene) $[NP(OC_6H_5)_2]_n$, which decomposes in concentrated sulfuric acid,[25] **I** was chemically very stable not showing signals of decomposition after several months. Pouring these solutions into water allowed the almost quantitative recovery of the polymer chemically unchanged (IR, ^1H and ^{13}C NMR spectra identical of those of **I**) with only a slight decrease in the analytical % C content (see Experimental Section). Also the glass transition temperatures were almost the same as that reported for **I** (159−162 °C). However, as in the HBF_4 and HCl experiments, the M_w of the new distributions were much lower and depended on the time of permanence in solution. The GPC chromatograms showed a marked decrease in M_w from 800 000 to 35 000 during the first hour and a much slower decrease to the final 17 000 during the following 3 months (see Experimental Section), but, in contrast with the HCl-promoted chain degradations, the distributions were much broader than the starting one with r reaching values of the order of 11 (see Experimental Section). In fact, the ^{31}P NMR spectrum showed that the strong single peak at −5.9 ppm (chloroform) was accompanied by a weak broad signal extended from −3 to −5 ppm and centered at −3.9 ppm, probably due to the lower molecular weight components of the distribution.

The stirring a suspension of **I** in aqueous concentrated nitric acid (63%) (where it was insoluble) for 1 or 24 h lead to almost identical results than the treatment with HBF_4 acid (only a degradation to average M_w of the order of 400 000), but at the refluxing temperature a complete decomposition with evolution of nitric oxides and formation of a clear yellowish solution was observed.

The protonation driven chain degradation of **I** is, therefore a cleaner process than the thermal and presumably it is related to the breaking of the protonated $P-HN-P^+-$ bonds (see Scheme 1) that should be less effective in heterogeneous systems (**I** is hydrophobic and its protonated form is not soluble in aqueous HCl). In the case of the sulfuric acid the degradation mechanism may be different as suggested by the higher complexity of the ^{31}P NMR spectrum. However, in all cases it is difficult to specify the exact nature of the new terminal groups resulting from the chain breaking, although, in the case of the polymers obtained from HCl, the terminal groups are very likely P−OH coming from the hydrolysis of P−Cl chain ends first generated during the acidic degradation. This might be supported by a weak very broadband near 3450 cm^{-1} observed in the IR spectrum of the samples **Ia** to **Id**, and also would explain that the hydrolysis of **I** in aqueous HCl that lead to the formation of free biphenol and ammonium dihydrogenophosphate is only effective after certain degree of the chain degradation.

In order to further understand the effects of the acidic degradation with HCl on the phosphazene chains, some molecular dynamics simulations were performed, followed by a complete experimental study of the solution properties of the polymers **Ia** to **Id**. The results are presented in the next sections.

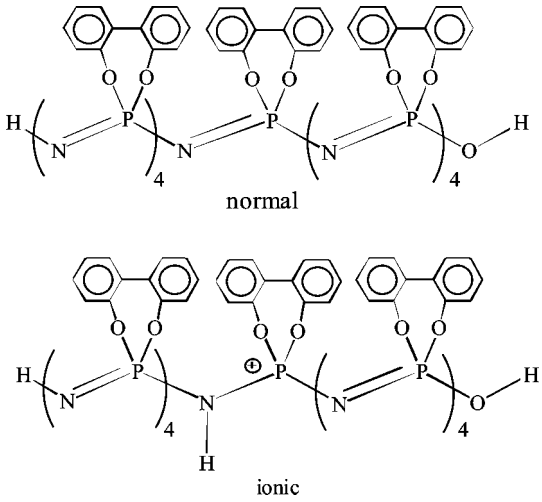

Figure 2. Sketches of the normal and ionic oligomers studied in this work. Ionic oligomer is supposed to be formed by protonation of one N atom followed by a migration of the positive charge to the P atom.

Table 1. Composition of the Systems Studied in This Work[a]

	normal oligomer	ionic oligomer	H^+	Cl^-	water
system A	1	0	200	200	5000
system B	0	1	199	200	5000

[a] Each system was packed into a cubic box having side length $L = 5.489$ nm (density of ca. 1 g cm^{-3}) and Periodic Boundary Conditions. Each system contained 200 molecules of HCl, but in the case of system B, one of the H^+ is incorporated to the oligomer.

Molecular Dynamics (MD) Simulations. *MD Software and Procedures.* The software (Amber,[26] NOPAC,[27] thermostat algorithm[28]) and computational strategy[29,30] employed in this work have been described before. Simulations were performed under Periodic Boundary Conditions at $T = 500$ K with an integration time step $\delta = 1$ fs (i.e., 1×10^{-15} s). After applying the equilibration procedure,[29,30] the data collecting stage consisted in 1.5×10^6 integration steps during which, the configuration of the system was saved at 10^3 integration steps intervals.

Molecular Systems. The basic molecule studied in this work is an H terminated oligomer containing nine repeating units of poly(2,2′-dioxy-1,1′-biphenyl)phosphazene. Two versions of this oligomer, having the structures sketched in Figure 2, were simulated. The first one is just a "normal" oligomer in which all the repeat units are identical. The second one, which will be called ionic, was supposed to be formed after an acid attack to the N−P bond of the central unit. This attack consisted on a protonation of the N atom followed by a migration of the positive charge to the P atom. Each one of these oligomers was packed into a cubic box having PBC together with 200 molecules of HCl and 5000 molecules of water, thus producing systems A and B, whose composition is summarized in Table 1. It is noteworthy to point out that both systems contain 200 molecules of HCl, although in system B, one on the protons was incorporated to the N−P bond.

Results. The goal of our analysis was to detect differences among the central units of the normal (system A) and ionic (system B) oligomers. Thus, distances from the central N and P atoms of each oligomer to the H^+, Cl^- ions and the water molecules (in fact to the O atom of the water molecule) contained in their respective systems were computed along the MD trajectories. These distances were employed to compute the radial correlation function $g(r)$ defined as the ratio between the probability of finding two particles at a distance $r \pm \delta r$ and the same probability computed assuming that the particles

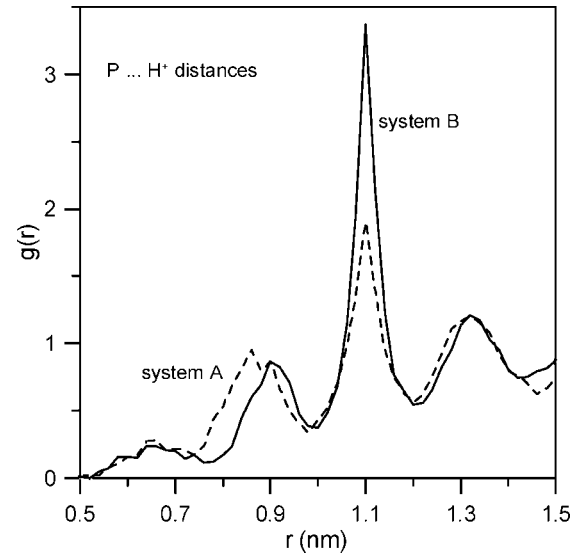

Figure 3. Radial correlation function $g(r)$ for the distances between P atom of the central unit of the oligomer contained in systems A (dash line) and B (solid line) and the H^+ ions. Systems A/B contains normal/ionic oligomers (see Table 1). Values of g/r) were computed from molecular dynamics trajectories performed at 500 K (see text for details).

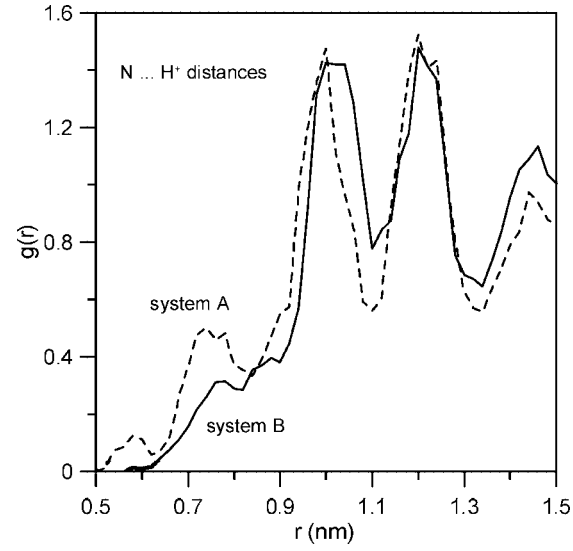

Figure 4. Same as Figure 3 for the distances N···H^+.

are randomly distributed. A value $\delta r = 0.01$ nm was employed in the present work. The values of the different g(r) functions are represented in Figures 3−8.

Correlation for distances P···H^+ and N···H^+ are shown, respectively, in Figures 3 and 4. According to these figures, positively charged H^+ get closer to either P or N atoms in the case of system A (i.e., normal oligomer) than in B (i.e., ionic oligomer). The differences are larger for N than for P atoms.

The correlation for distances to the negative Cl^- ions are represented in Figures 5 and 6 and show much stronger differences between system A and B than in the case of H^+. Thus, in the case of system A, practically there are no Cl^- ions within a distance of ca. 0.6 nm from either P or N atoms. On the contrary, in system B, the correlation functions show two sharp peaks at $r \approx 0.4$ and 0.6 nm.

Finally, the correlation for distances to the water molecules are represented in Figures 7 and 8 and exhibit a behavior similar to that of Cl^- ions in the sense that water molecules get into much closer proximity to both P and N atoms of the ionic

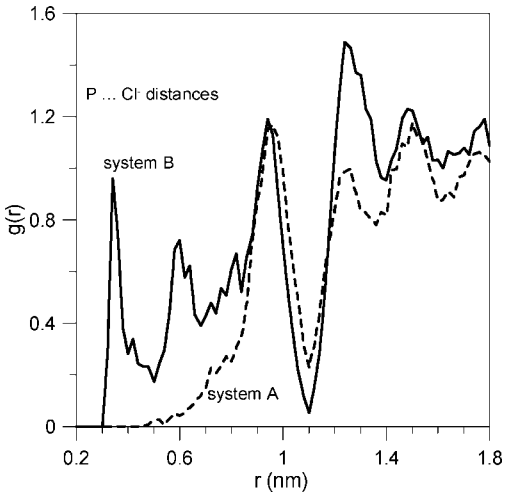

Figure 5. Same as Figure 3 for the distance P···Cl^-.

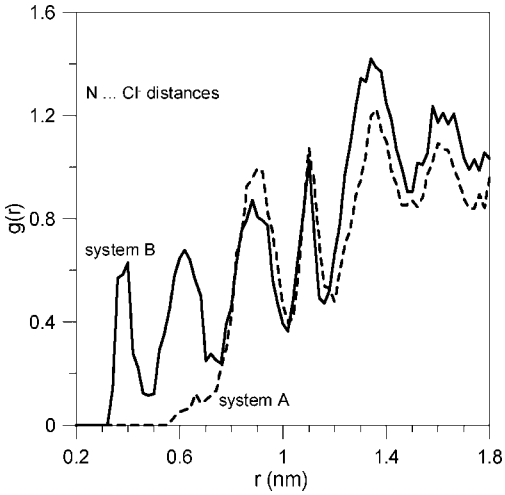

Figure 6. Same as Figure 3 for the distance N···Cl^-.

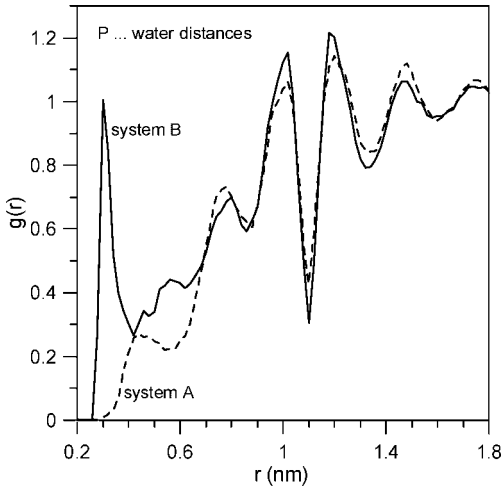

Figure 7. Same as Figure 3 for the distance P···water.

oligomer contained in system B than in their respective counterparts of the normal oligomer of system A.

It is interesting to notice the sharp peaks exhibited by all the solid lines in Figures 5–8 at $r \approx 0.3$ nm. They indicate that, once a given P−N bond has been protonated, the probabilities of finding the negative counterion of the acid or a water molecule at distances short enough as to produce a chemical

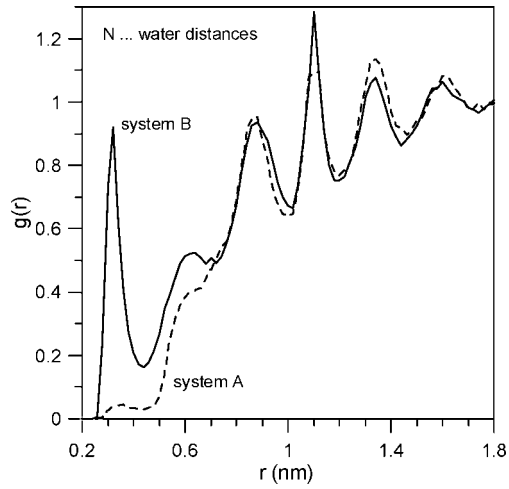

Figure 8. Same as Figure 3 for the distance N···water.

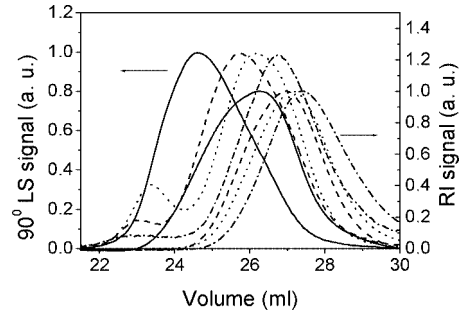

Figure 9. MALS signals at 90° and the RI signals for samples **Ia** (solid line), **Ib** (dashed line), **Ic** (dotted line) and **Id** (dash dotted line) obtained in a solution of 0.1% tetra-*n*-butylammonium bromide in THF.

reaction (hydrolysis) are noticeably increased as compared with equivalent probabilities in neutral P−N bonds.

SEC−MALS Results. The use of MALS together with a differential refraction index detector affords the measurement of molecular weight, concentration and radius of gyration of the polymer for the different slices of the chromatogram obtained, as it has been explained elsewhere.[31−33]

Figure 9 shows the differential refractive index, RI, signal and one of the light scattering signals (90°) for samples **Ia** to **Id**. The light scattering signals are proportional to the product of molecular weight and concentration, so they have a different shape than the RI signals that are proportional to concentration, and show a small shoulder at low elution volumes that correspond to polymer of high molecular weight. These shoulders appear at the same volumes as the original polymer (see figure 10) and they can be due to remains of the parent polymer that has not been degraded. However, the amount of polymer is negligible since the shoulders do not appear in the RI signal which depends only on concentration. Moreover, the chromatograms of the samples show no tails and, as expected, they displace to higher elution volumes as the time of the degradation treatment increases.

Figure 10 (lower part) depicts the logarithm of the molecular weight plotted versus the elution volume, i.e., absolute molecular weight calibration curves[34] of the degraded samples **Ia** to **Id** together with a sample of the same polymer **I** that has not been through any degradation reactions (in gray color). The calibration curves of the degraded samples are coincident, in the range they overlap, not only among themselves but also with that of the original polymer. The upper part of the figure shows the calibration curves of the radius of gyration of the same samples. The uncertainties in the radius of gyration for samples

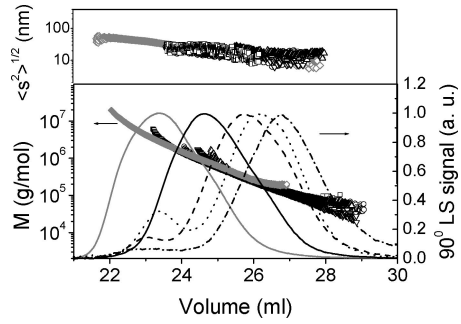

Figure 10. Lower part: Logarithm of molecular weight versus elution volume for samples **Ia** (□), **Ib** (○), **Ic** (▽), **Id** (△) and undegraded polymer (gray ◇) The MALS signal at 90° is also depicted (see caption of Figure 9). In gray solid line is shown the plot for the undegraded polymer. Upper part: Logarithm of squared root radius of gyration versus elution volume for the same samples.

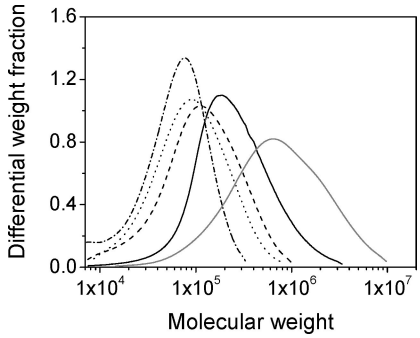

Figure 11. Differential molecular weight distributions. See captions of Figures 9 and 10.

Table 2. Averaged Molecular Weights, Polydispersities, and Scaling Parameters of Polyphosphazenes Obtained by Acidic Degradation with HCl

Degradation time	Sample	$10^{-5}M_w$ (g/mol)	M_w/M_n	q
10 min	**Ia**	3.78 ± 0.02	2.09 ± 0.01	0.38 ± 0.02
30 min	**Ib**	1.75 ± 0.03	1.80 ± 0.02	0.32 ± 0.04
1 h	**Ic**	1.41 ± 0.03	1.98 ± 0.03	0.3 ± 0.1
4 h	**Id**	0.86 ± 0.01	1.31 ± 0.05	0.3 ± 0.1

Ia to **Id** are larger than in molecular weight since the size of the polymer should be larger than $\lambda/20$ in order to notice the angular dependence of scattered light.[35] Despite this fact, Figure 10 clearly shows that the radius of gyration calibration curves of the degraded samples overlap with the non degraded polymer (in gray color). This behavior differs from the results obtained for the thermal degradation of the same polymer **I** in which the degraded samples had lower radius of gyration than the original nondegraded polyphosphazene of the same molecular weight.[4] Moreover, it supports the above-mentioned fact that the degradation with HCl is a cleaner process than the thermal one

The molecular weight distributions for the polymer fractions are presented in Figure 11. Mean values of molecular weights, polydispersities and standard deviations, are collected in Table 2.

Additional information on the polymer structure can be deduced from the study of the q parameter of the scaling law $\langle s^2\rangle^{1/2} = QM^q$ that relates radius of gyration and molecular weight.[36,37] The upper part of Figure 12 shows the scaling law for one of the samples, **Ia**, and the values of q for all the samples are presented in Table 2. The value of q reported for polymer **I** in THF is[4] 0.36 and the values obtained for the degraded samples are similar although affected by a greater error as a consequence of the imprecision in the radius of gyration mentioned above.

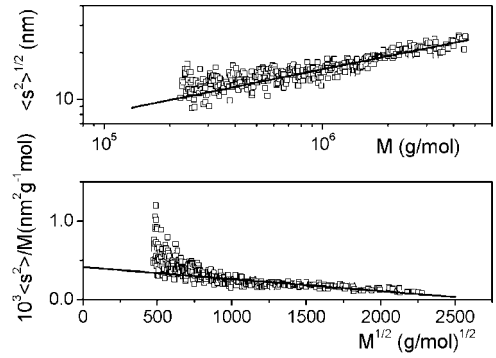

Figure 12. Log−log plot of root mean squared radius of gyration versus molecular weight, scaling law (upper part), and extrapolation to unperturbed dimensions (lower part) for polymer **Ia**.

The molecular dimensions of a polymer chain depend on the interactions with solvent molecules, thus the dimensions of the polymer under Θ conditions, or unperturbed dimensions, gave a better idea of the polymer behavior. The set of M and $\langle s^2\rangle$ values can be used to evaluate unperturbed dimensions.[38] According to the two parameters theory, the values of $\langle s^2\rangle/M$ versus $M^{1/2}$ should fit the following relationship:[39]

$$\frac{\langle s^2\rangle}{M} = \frac{\langle s^2\rangle_o}{M}(1 + AM^{1/2} + BM + \cdots)$$

and, with the omission of higher terms, the relationship is linear in $M^{1/2}$ with $\langle s^2\rangle_o/M$ as the independent term. The lower graph of Figure 12 shows the experimental values of $\langle s^2\rangle/M$ versus $M^{1/2}$ for the degraded sample of higher molecular weights, **Ia**. The negative slope exhibited by the extrapolation is a straight consequence of the under theta conditions of the system. Thus, the value of $\langle s^2\rangle/M$ will increase with decreasing M. The value of the intercept $(4.0 \pm 0.4) \times 10^{-4}$ nm^2 mol g^{-1} is similar to the one obtained for the parental polymer.[4] The unperturbed dimensions are customarily expressed as the characteristic ratio C_n that can be calculated from the value of $\langle s^2\rangle_o/M$ as:[36]

$$C_n = \frac{6M_o}{2l^2}\frac{\langle s^2\rangle_o}{M}$$

where l is the length of the PN bond and M_o the molecular weight of the repeating unit. The value obtained $C_n = 12$ is the same as the one obtained for the parental polymer **I** using the same technique SEC−MALS and calculated through molecular dynamics simulations.[4] It is worthwhile to point out that this behavior is different from that obtained for the thermal degraded samples[4] which presented values of $\langle s^2\rangle_o/M$ and thus values of C_n much smaller than those of the parental polymer. These smaller values of unperturbed dimensions were explained by the formation of a few very long branches produced during the thermal degradation.[4] The fact that the degraded samples of this work present both similar values of radius of gyration calibration curves, as explained above, and unperturbed dimensions than the parental polymer evidence the cleanness of the acidic degradation as compared with the thermal one.

Fluorescence Measurements. Figure 13 depicts the normalized (at the maximum of the emission band, 330 nm) emission spectra for degraded polymers (**Ia** through **Id**), the nondegraded one (**I**) and the 1,1′-biphenyl (used as the model compound) in dilute solutions of THF upon excitation of biphenyl groups at λ_{exc}= 280 nm. The **Ia**−**Id** samples exhibit similar spectra. However, the fluorescence spectra of **I** is slightly shifted to lower wavelengths perhaps due to the fact that this sample has a 0.02% of residual Cl atoms. Spectra show the absence of intramolecular excimers for any of the samples. The lack of intramolecular excimers, due to the angular orientation of both chromophore

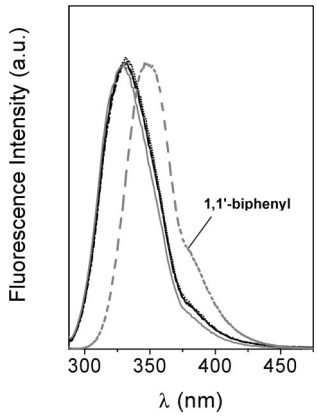

Figure 13. Emission spectra for samples **Ia** trough **Id** (black lines), undegraded polymer (I, gray line) and 1,1′-biphenyl used as model compound.

groups, has also been reported for other spiro polyphosphazenes containing binaphthoxy groups.[40] The nonstability of intermolecular excimers for 1,1′-biphenyl in solution was also described elsewhere.[41] The overall shape of the spectrum does not change between −5 through 45 °C, although there is an obvious decrease in the emission intensity with temperature. The Arrhenius plots show similar characteristics for all the polymer samples studied. Fluorescence quantum yields from degraded samples do not differ from those of the nondegraded one. Fluorescence intensity decays have also been obtained in THF at 25 °C upon selecting the maximum of emission (330 nm). Intensity profiles for all polymers were fit to the sum of two exponential decays. Two components in the 1.7−1.8 and 4.1−5.4 ns ranges, were obtained. The short-lived component, which contribution always represents more that 94% for any of the degraded and nondegraded polymers, was very similar to the lifetime obtained for the model compound (∼1.9 ns). These results noticeably differ from those obtained with other poly(binaphthoxyphospaze) homopolymers.[40] In the latter case the intramolecular energy transfer between binaphthoxy groups makes fluorescence decays much more complicated, thus profiles were fit to the sum of three-exponential terms. In the former one, chromophores in the chain behave rather independently of each other. The lifetime averages,[41] exhibit values in the range 1.8−2.0 ns for all **I** and **Ia**−**Id** polymer samples, which are very close to the lifetime for the model compound.

In an attempt to demonstrate the location of chromophores and find out more about the polymer microstructure, steady-state quenching experiments using nitrobenzene as the quencher were also carried out. The data were analyzed in terms of the Stern−Volmer equation.[19] Stern−Volmer plots, which were linear in the 0−0.12 mM quencher concentration range, exhibit similar slopes (K_{SV}). Bimolecular quenching constant (k_q) values for all the samples are in the 5900 ± 250 M^{-1} ns^{-1} range. Results also reveal identical behavior for all polymers, both degraded and nondegraded.

In brief, all our measurements of fluorescence suggest that all the degraded samples as well as the parental polymer have the same chemical structure, thus supporting the results obtained by SEC−MALS. However, it should be pointed out that the geometry of the biphenyl group that precludes the formation of intermolecular excimers and the absence of energy migration along the chain, dismisses the possibility of a more detailed analysis of the microstructure of these polymers.[42]

Conclusions

The acidic degradation of poly(2,2′-dioxy-1,1′-biphenyl)phosphazene consists on a protonation of some of the skeletal N atoms followed by a migration of the positive charge to a neighbor P atom and a posterior hydrolytical attack to those protonated bonds. Molecular Dynamics simulations indicate that only protonated P^+-NH bonds are hydrolyzed, leaving unaffected all the regular P−N skeletal bonds. Thus, the acidic hydrolysis seems to be a much more suitable procedure than the previously used thermal degradation to produce homogeneous samples with no noticeable cross-linking as the characterization of the hydrolyzed samples by means of SEC−MALS and fluorescence indicates.

Acknowledgment. We are grateful to the Spanish DGICYT (Projects MEC-04-CTQ2004-01484 and CTQ2005-04710/BQU) and CAM (Project S-055/MAT/0227), for financial support.

References and Notes

(1) De Jaeger, R.; Gleria, M. *Phosphazenes: A Worldwide Insight*; Nova Science Publishers: New York, 2004. Mark, J. E.; Allcock, H. R.; West, R. *Inorganic Polymers*; Prentice Hall: Englewood Cliffs; NJ, 1992. Allcock, H. R. *Chemistry and Applications of Polyphosphazenes*; Wiley: New York, 2002.
(2) Carriedo, G. A.; Fernández Catuxo, L.; García Alonso, F. J.; Gómez Elipe, P.; González, P. A. *Macromolecules* **1996**, *29*, 5320–5325.
(3) Carriedo, G. A. J. *Chil. Chem.* **2007**, *52*, 1190–5.
(4) Laguna, M. T. R.; Tarazona, M. P.; Carriedo, G. A.; García Alonso, F. J.; Fidalgo, J. I.; Saiz, E. *Macromolecules* **2002**, *35*, 7505–7515.
(5) Carriedo, G. A.; García Alonso, F. J.; González, P. A.; Menéndez, J. R. *J. Raman Spectrosc.* **1998**, *29*, 327–330.
(6) Carriedo, G. A.; Gómez-Elipe, P.; García Alonso, F. J.; Lizaso, E.; Muñoz, M. E.; Santamaría, A. *Macromol. Chem. Phys.* **2001**, *202*, 3437–3443.
(7) Búrdalo, J.; Tarazona, M. P.; Carriedo, G. A.; García Alonso, F. J.; González, P. A. *Polymer* **1999**, *40*, 4251–4257.
(8) Carriedo, G. A.; Fidalgo Martínez, J. I.; García Alonso, F. J.; Rodicio González, E.; Presa Soto, A. *Eur. J. Inorg. Chem.* **2002**, 1502–1510.
(9) Carriedo, G. A.; Fidalgo, J. I.; García Alonso, F. J.; Presa Soto, A.; Díaz Valenzuela, C.; Valenzuela, M. L. *Macromolecules* **2004**, *37*, 9431–9437.
(10) Carriedo, G. A.; García Alonso, F. J.; Díaz Valenzuela, C.; Valenzuela, M. L. *Macromolecules* **2005**, *38*, 3255–3262.
(11) Carriedo, G. A.; García Alonso, F. J.; González, P. A.; Gómez Elipe, P. *Polyhedron* **1999**, *18*, 2853–2859. Carriedo, G. A.; García Alonso, F. J.; González, P. A.; Díaz Valenzuela, C.; Yutronic, N. *Polyhedron* **2002**, *21*, 2579–2586. Carriedo, G. A.; García-Alonso, F. J.; García Alvarez, J. L.; Díaz Valenzuela, C.; Yutronic, N. *Polyhedron* **2002**, *21*, 2587–2592. Carriedo, G. A.; García Alonso, F. J.; Díaz Valenzuela, C.; Valenzuela, M. L. *Polyhedron* **2006**, *25*, 105–112.
(12) Carriedo, G. A.; Jiménez, J.; Gómez Elipe, P.; García Alonso, F. J. *Macromol. Rapid Commun.* **2001**, *22*, 444–447.
(13) Rojo, G.; Martín, G.; Agulló-López, F.; Carriedo, G. A.; García Alonso, F. J.; Fidalgo Martínez, J. I. *Chem. Mater.* **2000**, *12*, 3603–3610.
(14) Gutiérrrez Fernández, S.; Lobo-Castañón, M. J.; Miranda Ordieres, A. J.; Tuñón Blanco, P.; Carriedo, G. A.; García Alonso, F. J.; Fidalgo, J. I. *Electroanalysis* **2001**, *13*, 1399–1404.
(15) Allcock, H. R. *Appl. Organomet. Chem.* **1998**, *12*, 659–666.
(16) Allcock, H. R.; Fitzpatrick, R. J.; Salvati, L. *Chem. Mater.* **1991**, *3*, 1120–1132.
(17) Allcock, H. R. *Chem. Mater.* **1994**, *6*, 1476–1491.
(18) Tarazona, M. P.; Saiz, E. Solution Properties of Polyphosphazenes Determined by SEC−MALS and calculated by MD simulations. In *Synthesis and Characterizations of Poly(organo phosphazenes)*; Gleria, M., De Jaeger, R., Eds.; Nova Science Publishers: New York, 2004; Chapter 10; pp 211−235.
(19) Guillet, J. *Polymer Photophysics and Photochemistry: An Introduction to the Study of Photoprocesses in Macromolecules*; Cambridge University Press: Cambridge, U.K., 1985.
(20) Carriedo, G. A.; García Alonso, F. J.; Gómez-Elipe; P.; Fidalgo, J. I.; García Álvarez, J. L.; Presa Soto, A. *Chem. Eur. J.* **2003**, *9*, 3833–3836.
(21) O'Connor, D. V.; Ware, W. R.; André, J. C. *J. Phys. Chem.* **1979**, *83*, 1333–1343.
(22) Wisian-Neilson, P.; García Alonso, F. J. *Macromolecules* **1993**, *26*, 7156–7160.
(23) Wisian-Neilson, P.; Bahadur, M.; Iriarte, J. M.; Ford, R. R.; Wood, C. E. *Macromolecules* **1994**, *27*, 4471–4476.
(24) Maynard, S. J.; Sharp, T. R.; Haw, J. F. *Macromolecules* **1991**, *24*, 2794–2799.
(25) Allcock, H. R.; Kugel, R. L.; Valan, K. J. *Inorg. Chem.* **1966**, *5*, 1709–1715.

(26) http://www.amber.ucsf.edu/amber/amber.html; http://www.amber.ucsf.edu/amber/dbase.html; http://pharmacy.man.ac.uk/amber/
(27) MOPAC, *Quantum Chemistry Program Exchange*; Department of Chemistry, Indiana University: Bloomington, IN.
(28) Allen, M. P.; Tildesley, D. J. *Computer Simulation of Liquids*; Clarendon: Oxford, U.K., 1987.
(29) Marcelo, G.; Saiz, E.; Mendicuti, F.; Carriedo, G. A.; García Alonso, F. J.; García Alvarez, J. L. *Macromolecules* **2006**, *39*, 877–885.
(30) Carriedo, G. A.; Presa Soto, A.; Valenzuela, M. L.; Tarazona, M. P.; Saiz, E. *Macromolecules* **2008**, *41*, 1881–1885.
(31) Reed, W. F. in *Strategies in size exclusion chromatography*; Potschka, M., Dubin P. L., Eds.; American Chemical Society: Washington, DC, 1996; Chapter 2.
(32) Laguna, M. T. R.; Medrano, R.; Plana, M. P.; Tarazona, M. P. *J. Chromatogr. A* **2001**, *919*, 13–19.
(33) Tarazona, M. P.; Saiz, E. *J. Biochem. Biophys. Methods* **2003**, *56*, 95–116.
(34) Wyatt, P. J. *Anal. Chim. Acta* **1993**, *272*, 1–40.
(35) Huglin, M. B. Ed. *Light Scattering from Polymer Solutions*; Academic Press: London, 1972.
(36) Flory, P. J. *Statistical Mechanics of Chain Molecules*; Wiley: New York, 1969.
(37) De Gennes, P. G. *Scaling concepts in polymer physics*; Cornell University Press: Ithaca, NY, 1979.
(38) Búrdalo, J.; Medrano, R.; Saiz, E.; Tarazona, M. P. *Polymer* **2000**, *41*, 1615–1620.
(39) Yamakawa, H. *Macromolecules* **1993**, *26*, 5061–5066.
(40) Carriedo, G. A.; García Alvarez, J. L.; García Alonso, F. J.; Presa Soto, A.; Tarazona, M. P.; Mendicuti, F.; Marcelo, G. *Macromolecules* **2004**, *37*, 5437–5443.
(41) Cione, A. P. P.; Scaiano, J. C.; Neumann, M. G.; Gessner, F. *J. Photochem. Photobiol. A* **1998**, *118*, 205–209.
(42) Rabek, J. F. *Mechanism of Photophysical Processes and Photochemical Reactions in Polymers: Theory and Applications*; John Wiley & Sons: Chichester, U.K., 1987. Berlman, I. B. *Handbook of Fluorescence Spectra of Aromatic Molecules*, Academic Press: New York, 1973; p 176.

MA8015568